Peptidoglycan recycling mediated by an ABC transporter in the plant pathogen *Agrobacterium tumefaciens*

Michael C. Gilmore, Felipe Cava*

Laboratory for Molecular Infection Medicine Sweden (MIMS), Department of Molecular Biology, Umeå University, 90187 Umeå, Sweden

*For correspondence: felipe.cava@umu.se

Running title: Peptidoglycan recycling mediated by an ABC transporter

Keywords: bacterial cell wall, peptidoglycan recycling, *Agrobacterium tumefaciens*, Rhizobiales, ABC transporter

Abstract

During growth and division, the bacterial cell wall peptidoglycan (PG) is remodelled, a process which results in the liberation of soluble PG fragments called muropeptides. These fragments can be released to the environment, where they can have far-reaching consequences in signalling and interspecies interactions, or reinternalized and recycled by the cell. Bacteria belonging to the Rhizobiales and Rhodobacterales groups of the Alphaproteobacteria lack the canonical muropeptide transporter AmpG, despite encoding orthologs of the other key PG recycling enzymes AmpD and NagZ in their genomes. Using high-throughput transposon sequencing (Tn-Seq), we identified an alternative ATP-binding-casette (ABC) family transporter, YejBEF-YepA, which takes over this role in the Rhizobiales phytopathogen *Agrobacterium tumefaciens*. The broad-spectrum peptide transporter "core" YejBEF functions with a PG-specific periplasmic substrate-binding protein (SBP) YepA to transport muropeptides into the cytoplasm for recycling. Muropeptide import by YejBEF-YepA governs the expression of the β-lactamase AmpC in *A. tumefaciens* through an AmpR repression system, and its absence confers hypersensitivity to β-lactam antibiotics. However, we show that the absence of YejBEF-YepA causes severe cell wall defects that go beyond the lowered AmpC activity. Thus, contrary to previously established Gram-negative models, PG recycling is vital for cell wall integrity in *A. tumefaciens*. YepA is widespread in the Alphaproteobacteria including in many clinically and environmentally relevant bacteria, suggesting that YejBEF-YepA-mediated PG recycling could represent an important but overlooked aspect of cell wall biology in the Alphaproteobacteria.

Significance Statement

The cell wall is essential in most bacteria, and represents one of the most successful antibiotic targets. Recycling of peptidoglycan, the major cell wall component, has been thought to lack importance since its interruption has no known phenotypic consequences in *Escherichia coli*. Here, we identified a novel transporter for peptidoglycan recycling in the plant pathogen *Agrobacterium tumefaciens*. Surprisingly, peptidoglycan recycling seems to be vital for cell wall integrity in *A. tumefaciens*, since deleting the transporter results in severe cell wall defects and hypersensitivity to β-lactam antibiotics. Importantly, the transporter is widespread in the Alphaproteobacteria, a class which includes clinically relevant pathogens such as *Brucella abortus*, *Bartonella henselae* and *Ochrobactrum anthropi*, so could represent a promising antibiotic target in these bacteria.

46 # Introduction

47 The bacterial cell wall is composed primarily of peptidoglycan (PG), a
48 heteropolymer which consists of alternating *N*-acetylglucosamine (GlcNAc) and *N*-
49 acetylmuramic acid (MurNAc) sugars crosslinked by short peptide chains (1). In
50 order to facilitate growth and division, as well as adaption to environmental stressors,
51 the cell wall is constantly remodelled by an arsenal of lytic enzymes (2):
52 glucosaminidases and lysozyme cleave between the two sugars, endopeptidases
53 cleave within the peptide chains, carboxypeptidases cleave the C-terminal amino
54 acid from the peptide chains, amidases cleave the peptide chain from the MurNAc
55 sugar and lytic transglycosylases (LTs) cleave between the sugars with
56 simultaneous cyclisation of the terminal MurNAc to form 1,6-anhydroMurNAc. A
57 consequence of this remodelling activity is the liberation of peptidoglycan fragments,
58 termed muropeptides, which can be released into the environment where they can
59 have far-reaching consequences in signalling or interspecies interactions (3), or
60 imported into the cell for reuse in PG synthesis, in a process termed PG recycling
61 (4).

62 PG recycling has been well studied in some Gram-negative models. Typically,
63 anhydromuropeptides liberated by LTs are imported by the Major Facilitator
64 Superfamily (MFS) transporter AmpG (5), before being broken into their constituent
65 sugars and peptide by the amidase AmpD (6), β-hexosaminidase NagZ and LD-
66 carboxypeptidase LdcA (7) (Fig. 1A). Pathways exist for recycling both the
67 anhydroMurNAc and GlcNAc sugars (4, 8–10), while the peptide is directly
68 reincorporated into PG synthesis by ligation with UDP-MurNAc by the ligase Mpl
69 (11). Around 50% of the sacculus is turned over in *E. coli* per generation (12), but

only around 8% is released to the medium, due to recycling (13). Despite the extent of PG turnover, the abundance of proteins produced solely to enable PG recycling and its relatively wide conservation, its importance is unclear, since its interruption does not affect bacterial growth under laboratory conditions (4). The exception to this is a growth defect caused by the deletion of the LD-carboxypeptidase LdcA, which leads to a reduction in cell wall crosslinking due to the inability of tetrapeptide precursors to be used as a donor in the PG transpeptidation reaction (7, 14).

We noticed that Alphaproteobacteria belonging to the orders Rhizobiales and Rhodobacterales lack AmpG orthologs, despite encoding orthologs of other PG recycling enzymes such as AmpD and NagZ in their genomes. Using the plant pathogen *Agrobacterium tumefaciens* as model, we identified that the broad-specificity peptide ABC transporter YejBEF takes over the role of AmpG as muropeptide transporter in these bacteria, utilising an alternative PG-specific substrate-binding protein (SBP) YepA which is unique to the Alphaproteobacteria. PG recycling mediated by YejBEF-YepA governs expression of the β-lactamase AmpC through a canonical AmpR repression system, controlling β-lactam resistance in *A. tumefaciens* in place of AmpG. Importantly, we show that contrary to previously established Gram-negative models, PG recycling is vital for cell wall integrity in this bacterium since deleting the transporter results in significantly altered cell wall density and composition, leading to growth defects on low-osmolarity medium and hypersensitivity to β-lactam antibiotics in a manner partly independent of AmpC.

91 # Results

92 ## *A. tumefaciens* recycles PG

93 We first set out to determine if *A. tumefaciens* recycles PG, since it lacks an
94 ortholog of the PG recycling transporter AmpG. Since deletion of the
95 anhydromuramoyl-amidase AmpD results in the accumulation of
96 anhydromuramyltripeptides in the cytoplasm of *E. coli* (6), we deleted the *A.*
97 *tumefaciens* orthologs of both *ampD* (Atu2113) and *nagZ* (Atu1709) and used ultra-
98 performance liquid chromatography coupled to quadrupole-time of flight mass
99 spectrometry (UPLC-MS) to check for the accumulation of the substrates of these
100 enzymes in the cytoplasm (Fig 1B). We observed the accumulation of
101 anhydroMurNAc- and MurNAc-linked muropeptide species accumulating in the
102 cytoplasm of Δ*ampD*, while the GlcNAc-anhydroMurNAc and GlcNAc-MurNAc
103 disaccharides accumulated in the cytoplasm of Δ*nagZ*, confirming these enzymes
104 play the same respective roles in PG recycling in *A. tumefaciens* as in other Gram-
105 negative bacteria. Interestingly, we observed tri-, tetra- and pentapeptide
106 muropeptides accumulating in Δ*ampD*. In *E. coli*, typically only tripeptide
107 muropeptides are observed to accumulate in an *ampD* mutant due to the activity of
108 the LD-carboxypeptidase LdcA (6), suggesting that *A. tumefaciens* lacks this activity
109 in its cytoplasm. To confirm this, we ectopically expressed LdcA from *E. coli* in *A.*
110 *tumefaciens* on a plasmid, and observed a corresponding shift in accumulation from
111 tetrapeptide to tripeptide muropeptides (Fig S1). Additionally, trisaccharide
112 muropeptides also accumulated in Δ*ampD*, suggesting that *A. tumefaciens* can
113 transport dimers into its cytoplasm for recycling. The ion masses of these were
114 consistent with either crosslinked dimers or chains, but since LdcA expression
115 converted the di-tetrapeptide dimer into di-tripeptide (Fig. S1), they likely form chains

116 as the D-Ala is not crosslinked. Since *A. tumefaciens* does recycle PG, we reasoned
117 that it must have an alternative transporter of anhydromuropeptides.

118

119 Identification of the PG recycling transporter in *A. tumefaciens*

120 To identify the missing transporter, we took advantage of the antibiotic
121 Fosfomycin. This inhibits the first committed step of PG synthesis, the MurA-
122 catalysed conversion of UDP-GlcNAc into UDP-1-carboxyvinyl-GlcNAc, which forms
123 the substrate for the subsequent production of UDP-MurNAc by MurB (15). This step
124 can bypassed to some extent by the recycling of MurNAc, which confers higher
125 intrinsic resistance to Fosfomycin (8). We therefore used a high-throughput
126 transposon sequencing screen (Tn-Seq) to identify genes which are required for
127 survival under Fosfomycin treatment, reasoning that this should reveal genes
128 required for recycling MurNAc in *A. tumefaciens*, and thus our transporter. Our
129 Fosfomycin Tn-Seq screen revealed that recycling of MurNAc in *A. tumefaciens*
130 likely happens through the *Pseudomonas* pathway (8–10), using the enzymes AnmK
131 (Atu1827), MupP (Atu1614), AmgK (Atu0026) and MurU (Atu0025) to process
132 anhydroMurNAc and convert it into UDP-MurNAc for reuse (Supplementary Data 1).
133 In the list of genes which were statistically underrepresented in transposon insertions
134 with 2 mg/mL Fosfomycin (Fig. 2A, Supplementary Data 1), there were two ATP-
135 binding cassette (ABC) transporters. One consisted of the membrane-spanning and
136 nucleotide-binding proteins of the phosphonate ABC importer *phnJK*, which is
137 reported to form part of the carbon-phosphorus (C-P) lyase machinery (16, 17).
138 Since this complex mediates the cleavage of C-P bonds, such as that found in
139 Fosfomycin, it likely confers resistance to Fosfomycin by degrading it. Indeed,
140 degradation of Fosfomycin by Rhizobiales bacteria has been previously observed

141 (18), and this process could explain the relatively high intrinsic Fosfomycin
142 resistance in *A. tumefaciens*. The other ABC transporter with significantly reduced
143 Tn insertions was a putative peptide ABC importer previously reported as YejBEF
144 (Fig. 2A) consisting of two membrane-spanning proteins *yejB* and *yejE* (Atu0188 and
145 Atu0189) and an ATPase *yejF* (Atu0190). Interestingly, these genes form an operon
146 with a periplasmic substrate-binding protein (SBP), *yejA* (Atu0187) which was not
147 affected in Tn insertions under Fosfomycin treatment. Instead, our screen identified
148 an alternative peptide-binding SBP (Atu1774) with significantly fewer Tn insertions,
149 which showed sequence similarity to *yejA* (38.7% identity). The YejABEF ABC
150 transporter has previously been reported as a broad-specificity peptide importer
151 required for resistance to plant antimicrobial peptides and proper bacteroid
152 differentiation in *Sinorhizobium meliloti* (19, 20), and thus together with the SBP
153 Atu1774, represented a good candidate for an importer of muropeptides.

154 To investigate whether YejABEF constitutes a novel PG recycling transporter
155 in *A. tumefaciens*, we deleted the full operon corresponding to *yejABEF* (Atu0187-
156 atu0190) (Fig 2C) and used UPLC to check the supernatant of this mutant for the
157 accumulation of PG fragments. As would be expected, anhydromuramyl tri-, tetra-
158 and peptapeptides accumulated in large quantities in the extracellular milieu of the
159 Δ*yejABEF* mutant (Fig. 2B). Since deletion of *ampD* results in the accumulation of
160 muropeptides in the cytoplasm of *A. tumefaciens*, we reasoned that deletion of the
161 transporter in a Δ*ampD* background must necessarily prevent this. We therefore
162 checked the cytoplasmic soluble muropeptides in a Δ*yejABEF*Δ*ampD* mutant (Fig.
163 2D) using UPLC. There was no cytoplasmic muropeptide accumulation in the double
164 mutant, indicating that YejABEF is the sole transporter responsible for muropeptide
165 recycling in *A. tumefaciens*. Further, ectopic expression of the known MFS

166 muropeptide importer AmpG from *E. coli* restored the cytosolic accumulation of
167 muropeptides in the Δ*yejABEF*Δ*ampD* background (Fig. S2), confirming that these
168 transporters have the same function. Finally, we produced anhydro-disaccharide
169 tetrapeptides with the non-canonical D-amino acid D-Met instead of D-Ala in the
170 fourth position ($M4N^{Met}$) as a probe for PG recycling (14). Δ*ampD* cultures
171 exogenously supplemented with $M4N^{Met}$ yielded an accumulation of
172 anhydroMurNAc-$P4^{Met}$ (i.e., $M4N^{Met}$ processed by NagZ) in the cytoplasm (Fig. 2E),
173 which did not occur in the Δ*yejABEF*Δ*ampD* mutant, further confirming the
174 requirement of YejABEF for the import of anhydromuropeptides into the cytoplasm.

175

176 Role of PG recycling in β-lactam resistance in *A. tumefaciens*

177 *A. tumefaciens* encodes a canonical inducible AmpC β-lactamase system
178 where the import of anhydromuropeptides controls β-lactamase expression through
179 the regulator AmpR (21, 22)(Fig. 3A). We therefore reasoned that the Δ*yejABEF*
180 mutant could show decreased Amp resistance through lower β-lactamase
181 expression. Indeed, we observed a >250-fold decrease in Amp MIC in the
182 transporter mutant (Fig. 3B). Consistently, hydrolysis of the chromogenic
183 cephalosporin nitrocefin was decreased considerably in the mutant, indicating lower
184 AmpC activity (Fig. 3C).

185 Interestingly, the three parts of the transporter that are required for
186 Fosfomycin resistance form a cluster with the putative SBP YejA (Atu0187). Using
187 RT-PCR, we confirmed that *yejA* is co-expressed with *yejBEF* on a single mRNA
188 (Fig. S3A). As mentioned, Tn insertions in *yejA* were not significantly reduced under
189 Fosfomycin treatment. Instead, we found that mutation of the *yejA* paralog Atu1774

190 conferred Fosfomycin sensitivity. To investigate the potential role of these SBPs, we
191 generated single mutants of *yejA* and Atu1774 and compared them with mutants of
192 other parts of the transporter (Fig. 3C). The ampicillin sensitivity of the Δ*yejB*, Δ*yejE*,
193 Δ*yejF* and ΔAtu1774 mutants recapitulated that of the entire operon deletion mutant
194 (Fig. S3B), indicating that these components are required for the PG recycling
195 function of the transporter, while the Δ*yejA* mutant was phenotypically identical to the
196 WT. Additionally, we observed the accumulation of PG fragments in the supernatant
197 of ΔAtu1774 on the same levels as for Δ*yejABEF*, while Δ*yejA* again reflected the
198 WT (Fig. 3E). Collectively these results demonstrate that Atu1774, instead of YejA, is
199 the SBP involved in PG recycling in *A. tumefaciens*, and so we renamed it YepA for
200 Yej-peptidoglycan binding protein A.

201 Remarkably, we noticed that Δ*yejABEF* and the single mutants Δ*yejB,* Δ*yejE,*
202 Δ*yejF and* Δ*yepA* were more Amp sensitive than Δ*ampC* (Fig. 3B), meaning that the
203 Amp hypersensitivity of the PG recycling defective mutants was not just a result of
204 decreased β-lactamase activity. Indeed, the nitrocefin hydrolysis assay showed that
205 Δ*yejABEF* retained more β-lactamase activity than Δ*ampC* despite its lower Amp
206 resistance (Fig. 3C). This was further confirmed by testing sensitivity of both mutants
207 to aztreonam, a monobactam β-lactam antibiotic. The Δ*ampC* mutant showed an
208 identical resistance profile to the WT, suggesting that AmpC plays no role in
209 resistance of *A. tumefaciens* to aztreonam, while Δ*yejABEF* was once again
210 hypersensitive (Fig. 3F).

211

PG recycling is required for cell wall integrity in *A. tumefaciens*

We therefore hypothesised that the absence of YejBEF might cause cell wall defects which result in increased sensitivity to β-lactam antibiotics. To challenge cell wall strength, we first grew the mutant and WT strains in LB with no added NaCl (LB_0) to see how growth would be affected by low-osmolarity conditions. The Δ*yejB* mutant (phenotypically identical to the total Δ*yejABEF* mutant) displayed cell swelling and lysis (Fig. 4A), while the Δ*yejABEF* and Δ*yepA* mutants (but not Δ*yejA*) had a severe growth defect (Fig. 4B, S4A) which indicated a compromised cell wall. To investigate this further, we chemically analysed the cell wall of the Δ*yejB* mutant and WT using UPLC. While total crosslinking was slightly decreased in the mutant (Fig. 4C), interestingly, LD-crosslinking was more affected than DD-crosslinking, which was actually slightly higher relative to the WT. Since LD-transpeptidases are not affected by most β-lactam antibiotics (23), a higher dependence of the Δ*yejABEF* mutant on PBPs for PG crosslinking could be a possible contributing factor to its decreased β-lactam tolerance. Importantly, the total amount of PG in the mutant, as determined by the area under the whole chromatogram normalized to the optical density of the culture, was decreased considerably (Fig. 4D), suggesting that PG biogenesis was compromised. Quantification of the primary soluble cytoplasmic PG precursor UDP-muramylpentapeptide (UDP-M5) showed a corresponding decrease (Fig. 4E), indicating that PG recycling is an important source of material for PG synthesis in *A. tumefaciens*.

To further investigate the cell wall defects of Δ*yejABEF*, we used Tn-Seq to identify genes which confer greater or reduced fitness to the mutant when interrupted by Tn insertion (Fig 4F, 4G, Supplementary Data 2). Consistent with the observed defects of Δ*yejABEF* in PG synthesis and crosslinking, we found that synthetically

237 detrimental mutants included a putative LD-transpeptidase (Atu1615), bifunctional
238 PBP (Atu0931), DD-carboxypeptidase (Atu1499), and lytic transglycosylases MltB
239 (Atu3779), MltG (Atu1099) and RlpA (Atu1500), suggesting that additive effects
240 caused by the loss of these PG synthesis and remodelling proteins in combination
241 with PG recycling results in loss of fitness or non-viability. These results were
242 recapitulated by a second Tn-Seq comparing insertions in the Δ*yepA* and Δ*yejA*
243 mutants (Fig. S4B).

244 Conversely, mutations in several glycosyltransferases (Atu2583, Atu2590,
245 Atu2592), a UDP-GlcNAc dehydrogenase (Atu2582) and a putative ABC exporter
246 (Atu2577) improved fitness of the Δ*yejABEF* mutant. These genes form part of a
247 cluster likely to be involved in the synthesis of an uncharacterized glycan, previously
248 reported to be required for resistance to phenazines in *A. tumefaciens* (24). Since its
249 synthesis seems to use UDP-GlcNAc as a building block, we hypothesized that
250 these mutations might redirect GlcNAc flux to PG synthesis, thereby improving
251 Δ*yejABEF* fitness. However, this does not seem to be the case, as measured UDP-
252 M5 and UDP-MurNAc levels in ΔAtu2582 and ΔAtu2582Δ*yejABEF* strains showed
253 no differences to their WT and Δ*yejABEF* counterparts (Fig. S4C). It remains to be
254 seen what role this polymer plays in cell wall biology in *A. tumefaciens*.

255

256 YejBEF-YepA is conserved in the Rhizobiales and Rhodobacterales
257 orders of the Alphaproteobacteria

258 Finally, to define the degree of conservation of the PG recycling function of
259 YejBEF in bacteria, we generated a molecular fingerprint that allowed us to
260 differentiate between YepA and YejA. Using the JDet package (25), we generated a

261 set of specificity-determining residues from an alignment of YejA and YepA orthologs
262 (Fig. 5B). While YejABEF is broadly conserved across the proteobacteria, YepA is
263 exclusive to the Alphaproteobacteria (Fig 5A), being present in almost all families in
264 the Rhizobiales and Rhodobacterales orders, which also mostly lack AmpG. These
265 bacteria inhabit a broad spectrum of niches including plant symbionts and pathogens
266 (Rhizobiales), mammalian pathogens (Brucellaceae, Bartonellaceae), soil bacteria
267 (Azospirilliceae) and photosynthetic marine bacteria (Rhodobacteriaceae)
268 suggesting that YejBEF-YepA is not associated with one particular lifestyle.
269 Interestingly, while most species opt either for AmpG or YejBEF-YepA, these PG
270 transporters seem to coexist in a number of species such as in the
271 Bradyrhizobiaceae indicating that one or both could be used under different
272 conditions.

273

274 Discussion

275 PG biosynthesis and remodelling have been the subject of decades of research, but
276 the focus on relatively few model organisms has left the diversity of these processes
277 poorly understood. This particularly applies to PG recycling, which has additionally
278 suffered from a perceived lack of importance, since its interruption in the Gram-
279 negative model organism *E. coli* has no detrimental effect to the bacterium under lab
280 conditions (4). Muropeptides are a unique molecular signature of bacteria which are
281 highly immunogenic (26) and often mediate interspecies interactions (3). Therefore,
282 PG recycling is a factor which influences bacterial virulence and immune response
283 activation (27–29). Additionally, the high turnover of PG during the cell cycle means
284 that significant amounts of material would be lost if it were not recycled. Many

285 bacteria outside the typical models lack orthologs of key PG recycling enzymes, but
286 have others (4), suggesting there are alternative enzymes or pathways to be
287 discovered. For example, it was recently uncovered that both *Vibrio cholerae* (14)
288 and *Acinetobacter baumanii* (30, 31) have different functional analogs of the *E. coli*
289 LD-carboxypeptidase LdcA with a separate but convergent evolution. We noticed
290 that many bacteria belonging to the Rhizobiales and Rhodobacterales orders of the
291 Alphaproteobacteria lacked an AmpG transporter despite having orthologs of the
292 other key PG recycling enzymes AmpD and NagZ. Using the plant pathogen *A.*
293 *tumefaciens* as model, we identified an alternative ABC transporter that takes over
294 this role. *A. tumefaciens* is a fascinating model to study the growth and division of
295 bacteria, because it exhibits an unusual asymmetric polar growth mode, and relies
296 heavily on the typically dispensable LD-transpeptidases for peptidoglycan
297 crosslinking (32).

298 What happens to the PG after it is transported into the cell? An interesting
299 difference between muropeptide recycling in *A. tumefaciens* and *E. coli* is the variety
300 of intracellular muropeptide species which accumulate in the Δ*ampD* mutant. In *E.*
301 *coli*, only the NagZ- and LdcA-processed anhydromuramyl tripeptide accumulates on
302 significant levels (5), whereas in our *A. tumefaciens* Δ*ampD* mutant, peaks
303 corresponding to a wide variety of anhydromuramyl tri-, tetra- and pentapeptides are
304 present as well as dimeric muropeptides (Fig. 1B). Since direct recycling of
305 tetrapeptide precursors is typically highly toxic to the cell (7, 14), and we were unable
306 to detect UDP-M4^{Met} on treating *A. tumefaciens* with M4N^{Met} (Fig. 2E), we suggest
307 that *A. tumefaciens* does not directly reuse the PG peptide by ligation with UDP-
308 MurNAc as in some other Gram-negative bacteria. Instead, it might simply degrade
309 the released peptides and reincorporate the released amino acids into *de novo*

310 precursor synthesis or use them as a source of C or N. This idea is supported by the
311 lack of Mpl ligase or LD-carboxypeptidase orthologs in *A. tumefaciens*, and by the
312 genetic context of *yejABEF* since it clusters with a putative D-alanine dehydrogenase
313 *dadA* (Atu0192, labelled as a pseudogene due to a frameshift mutation, but this
314 occurs after the catalytic domain suggesting that it could have retained its activity)
315 and glutamine synthetase *glnA* (Atu0193) which uses glutamate as a substrate.

316 It is interesting that the PG SBP YepA is located separately from the rest of
317 the transporter in the genome. This raises the possibility of separate transcriptional
318 regulation of the "core" and PG-binding parts of the transporter, which would allow its
319 PG recycling function to be regulated independently of its function as a broad-
320 spectrum peptide importer. Additionally, the presence of two SBPs competing for the
321 same core could allow regulation of transporter function at the protein level, since
322 higher levels of one SBP might be expected to preclude binding of the other. YepA
323 also seems to have a conserved position beside a both a predicted cytoplasmic
324 DsbA-like protein (Atu1775) of unknown function and the essential periplasmic polar
325 growth protein RgsG (33), but the function of these two genes remains to be
326 identified.

327 The presence of an AmpC induction system based on released muropeptides
328 has been previously reported in *A. tumefaciens* (21), but the mechanism through
329 which muropeptides enter the cell has not been revealed until now. As a soil
330 bacterium, *A. tumefaciens* likely encounters β-lactam antibiotics in the environment,
331 so the presence of an inducible β-lactamase system could be a way to counter
332 these. However, although YejABEF does control the induction of AmpC, we showed
333 that its effect on β-lactam sensitivity is also partly caused by cell wall defects which
334 occur in its absence. The requirement of YejABEF for cell wall integrity and normal

growth was surprising, since *E. coli* has been shown to have no physiological defects on deletion of AmpG (4). Our Tn-Seq screen in Δ*yejABEF* revealed synthetically lethal cell wall-related genes including a bifunctional PBP, an LD-transpeptidase, and three LTs. Insertions in the synthetic PBP and LD-transpeptidase could result in lethality due to additive effects on top of the synthesis defects that already occur. Mutation of LTs is known to cause periplasmic stress due to periplasmic crowding caused by the accumulation of PG chains (34). Interruption of PG recycling could exacerbate periplasmic crowding, since we observed PG fragments accumulating in large amounts in the supernatant of Δ*yejABEF*. That we observe chains accumulating in the cytoplasm of Δ*ampD* but not in the supernatant of Δ*yejABEF* suggests they could be too large to escape the outer membrane, accumulating in the periplasm and thereby causing osmotic stress.

Our Tn-Seq screen also revealed that Tn insertions in a gene cluster likely responsible for the synthesis of an uncharacterised glycan alleviated the fitness cost of deleting Δ*yejABEF*. While this could be consistent with the idea of alleviating periplasmic crowding, *A. tumefaciens* also produces osmoregulated cyclic β-glucans (35), which did not show up in our screen, meaning this is likely not the case. This polymer has previously been reported as required for tolerance of the phenazine pyocyanin in *A. tumefaciens* (24), suggesting it could play some role in oxidative stress metabolism. Cell wall defects have previously been associated with an overproduction of hydroxyl radicals (36), and the potential role of YejABEF in periplasmic oxidative stress is a subject for future research.

YejABEF has previously been reported as important for proper bacteroid differentiation and resistance to the plant antimicrobial peptide NCR247 in *S. meliloti* (20, 37). Though this was thought to be due to its activity as a promiscuous peptide

360 importer, we suggest that it actually comes from its function as a PG transporter,
361 since AmpD is also required for NCR247 tolerance and the non-PG SBP YejA is not
362 (37). Indeed, the bacteroids formed by *S. meliloti* Δ*yejE* and Δ*yejF* mutants (20)
363 share strikingly similar aberrant morphologies with our Δ*yejABEF* mutant grown on
364 low osmolarity medium (LB_0, Fig. 4A) indicating that PG recycling is necessary to
365 maintain cell wall integrity in *S. meliloti* during bacteroid differentiation. *A.*
366 *tumefaciens*, along with *Brucella abortus* and *Bartonella henselae*, is an intracellular
367 pathogen, and so "hiding" its released PG from the host could be an essential
368 strategy to avoid immune detection particularly since immune receptors for PG are
369 located intracellularly. The effect of the transporter on virulence and immune
370 response evasion in other related species remains to be studied, but the widespread
371 presence of YepA in the Alphaproteobacteria and its physiological importance to *A.*
372 *tumefaciens* suggests that PG recycling could be an important and overlooked
373 aspect of cell wall biology in these bacteria.

374 The question of why *A. tumefaciens* uses an ABC transporter to recycle PG
375 instead of a PMF-dependent MFS transporter such as AmpG remains. The use of
376 different energy sources could mean that PG recycling is required by *A. tumefaciens*
377 under a specific condition where ATP is available as an energy source but
378 membrane polarisation is affected. However, *yepA* does not seem to be limited to
379 any one particular niche, being present in diverse plant and animal pathogens and
380 symbionts also environmental and marine bacteria (Fig. 5). The Rhizobiales are
381 known to be particularly rich in ABC transporters, with 146 full ABC importers
382 present in *Sinorhizobium meliloti* (38, 39). One possible reason for this is that it could
383 facilitate a common mechanism of regulation of transport. Inactivation of ABC
384 transporters on a cellular scale has been identified previously in *Rhizobium*

385 *leguminosarum* in response to sensing of global cellular nitrogen availability (40–42)
386 or glutathione levels (43), through a putatively post-translational mechanism which
387 remains to be elucidated (40, 42). Therefore, using an ABC transporter for PG
388 recycling could allow the cell to coordinate the regulation of this process with the
389 regulation of acquisition of other nutrients and energy sources, perhaps in
390 synchronisation with the cell cycle since glutathione levels are known to fluctuate
391 during the cell cycle in the related Alphaproteobacterium *Caulobacter crescentus*
392 (44).

393

394 # Methods

395 ## Strains and Growth Conditions

396 Strains used in this study are listed in Table S1. *A. tumefaciens* strains were
397 grown in LB, ATGN or ATSN (prepared as ref. (45) but without the addition of $FeSO_4$
398 to avoid precipitation as its absence did not affect growth) at 30°C unless stated
399 otherwise. *E. coli* strains were grown in LB at 37°C. All *A. tumefaciens* mutants are
400 derivatives of the *Agrobacterium fabrum* strain C58. When required, antibiotics were
401 added to growth media: Kanamycin (50 µg/mL *E. coli*, 300 µg/mL *A. tumefaciens*),
402 Ampicillin (100 µg/mL) or Chloramphenicol (20 µg/mL). Growth curves were done
403 using a microplate reader (Eon Biotek) to measure OD_{600} of 200 µL cultures in a 96-
404 well microplate over 28h at 5 minute intervals. Three technical replicates of three
405 biological replicates (i.e. separate parental cultures) were used per condition. Initial
406 cultures were prepared by adjusting exponentially growing cultures to OD_{600} 0.01.

407

408 ## Construction of Plasmids and Mutants

409 Expression and allelic exchange vectors were constructed using the primers
410 outlined in Table S2. Allelic exchange vectors for *A. tumefaciens* were constructed
411 using isothermal assembly of flanking regions with the suicide vector pNPTS139;
412 mutagenesis was carried out as described (46). Protein expression vectors were
413 constructed by PCR of the region of interest with addition of restriction sites by
414 primers, then restriction digest and ligation before transformation into *E. coli* DH5α.

415

416 ## Antibiotic Resistance Determination

417 Resistance to various antibiotics was determined on agar using MIC Test
418 Strips (Liofilchem). Exponential cultures were adjusted to OD_{600} 0.1 in PBS before
419 being spread across an LB agar plate three times using a sterile cotton swab; the
420 plate was rotated 60° between each spreading. The strip was applied once the plate
421 had dried fully.

422

423 ## Nitrocefin Hydrolysis Assay

424 Overnight cultures of *A. tumefaciens* strains were diluted 1:3 in fresh LB with 50
425 μg/mL ampicillin added (to induce *ampC* expression) and grown for 1 h. 1 mL of
426 culture normalised to OD_{600} 0.4 was prepared which was pelleted and washed in 1
427 mL of PBS. The final pellet was then resuspended in 1 mL lysis buffer (PBS with
428 0.2% Triton X-100, 50 μg/mL lysozyme and 2 mM EDTA) and incubated on ice for 30
429 min to lyse the cells. 200 μL reactions were set up containing 100 μL lysate, 96 μL
430 PBS and 4 μL 500 μg/mL nitrocefin (Oxoid) and the reaction was followed by
431 monitoring A_{486} for 2 h in a microplate reader (Eon Biotek) with readings every 5 min.

432

433 Soluble muropeptide analysis

434 To determine the presence and levels of intra- and extracellular soluble
435 muropeptides, bacteria were grown until late exponential phase (roughly OD600 0.7)
436 in minimal media before being cooled on ice for 10 min and normalised to the same
437 OD_{600}. Cells were then harvested by centrifugation at 10,000 × g for 2 min. The
438 supernatant was decanted and passed through a 0.22 µm filter, then boiled for 10
439 min, centrifuged at maximum speed in a benchtop centrifuge for 10 min to remove
440 precipitated proteins and concentrated 20 times in a SpeedVac system. Meanwhile,
441 the cell pellet was washed three times in ice-cold 0.9% NaCl, resuspended in 0.9%
442 NaCl so that the cells are 20 times concentrated and boiled for 10 minutes before
443 centrifugation at maximum speed in a benchtop centrifuge for 10 min to remove the
444 proteins and insoluble fraction.

445 Detection and chemical characterisation of the soluble muropeptides was
446 carried out using an Acquity H-Class UPLC (Waters) coupled to a Xevo G2/XS
447 QTOF mass spectrometer. Chromatographic separation was achieved using an
448 Acquity UPLC BEH C18 column (Waters) maintained at 45°C. A linear gradient of
449 0.1% formic acid in water to 0.1% formic acid in acetonitrile was used for elution. UV
450 detection was performed at 204 nm. The QTOF instrument was operated in positive
451 ion mode, with data collection performed in untargeted MS^e mode. The parameters
452 were set as follows: capillary voltage 3.0 kV, source temperature 120°C, desolvation
453 temperature 350°C, sample cone voltage 40 V, cone gas flow 100 L h^{-1} and
454 desolvation gas flow 500 L h^{-1}. Data acquisition and processing was performed using
455 the UNIFI software (Waters). A compound library of expected muropeptides was built
456 in UNIFI by drawing the structures in ChemSketch (http://www.acdlabs.com). This

457 library was used for automated processing of the data and quantification by
458 integration of the peaks from extracted ion chromatograms.
459

460 ## Peptidoglycan Analysis

461 Peptidoglycan isolation and analysis were carried out as described previously
462 (47). Briefly, 10 mL stationary phase cultures were normalised to the same OD_{600},
463 pelleted, resuspended in 5% SDS and boiled for 2 h with stirring. The obtained
464 sacculi were washed repeatedly in water to remove the SDS before analysis;
465 pelleting was performed by ultracentrifugation in an Optima MAX-TL benchtop
466 ultracentrifuge at 150,000 x g. The final pellet was resuspended in water and
467 digested overnight with muramidase (80 µg/mL) before adjustment to pH 9.5 with
468 addition of 0.5 M sodium borate, reduction with addition of 10 mg/mL sodium
469 borohydride for 20 min at RT and adjustment to pH 3.5 by addition of
470 orthophosphoric acid.

471 Liquid chromatography was carried out using an Acquity H-Class UPLC
472 system (Waters) equipped with an Acquity UPLC BEH C18 column (2.1mm x 150
473 mm, 130 Å pore size and 1.7 µm particle size, Waters). Chromatographic separation
474 was achieved using a linear gradient from 0.1% formic acid in water to 0.1% formic
475 acid in acetonitrile. Peaks were identified by running a reference sample in LC-MS
476 using the same method as above and assigning peak identities using retention time.
477 The relative amount of each muropeptide was calculated by integrating all the peaks
478 and dividing each peak area by the total area of the chromatogram, while the total
479 area of the chromatogram was taken as the relative density of PG per sample and
480 expressed relative to the WT.

481

482 M4N^{Met} incorporation experiment

483 M4N was prepared by digesting purified *V. cholerae* sacculi using the lytic
484 transglycosylase MltA. An in vitro Ldt-mediated exchange reaction with purified LdtA
485 was used to swap the D-Ala in position 4 with D-Met to produce M4N^{Met} as described
486 (48). 10 mL of exponentially growing *A. tumefaciens* cultures was pelleted and
487 resuspended in 200 µL fresh medium, and approximately 15 µg M4N^{Met} was added
488 to each. The cultures were then grown for a further hour and prepared for soluble
489 precursor analysis as described above.

490

491 Bioinformatic Analyses

492 Sequences of SBPs corresponding to YejA and YepA were identified in
493 representative species spanning the Rhizobiales and Rhodobacterales orders of the
494 Alphaproteobacteria: *A. tumefaciens*, *Sinorhizobium meliloti*, *Bartonella henselae*,
495 *Brucella melitensis*, *Ochrobactrum anthropi*, *Dinoroseobacter shibae* and
496 *Phaeobacter inhibens*. SBPs were identified by phenotype for *D. shibae* and *P.*
497 *inhibens* (using FitnessBrowser (49) to look for the SBP with the expected β-lactam
498 and Fosfomycin sensitivity phenotypes) and eggNOG 5.0 (50) using fine-grained
499 orthologs of Atu1774 and Atu0187 for the others. Sequences were aligned using
500 MUSCLE (51) and the JDet package (25) was used to find specificity-determining
501 positions (SDPs), which were visualised using WebLogo (52). To produce a
502 phylogenetic tree, all YejA orthologs were downloaded from OrthoDB (53), aligned
503 using MUSCLE v5 and the previously determined SDPs were used to label each as
504 either YejA or YepA. AmpG orthologs from OrthoDB were filtered by BLASTP

505 against *E. coli* AmpG using an E value cutoff of $1x10^{-25}$. PhyloT was used to produce
506 a phylogenetic tree of all species on OrthoDB and orthologs of YejA, YepA and
507 AmpG were mapped against this. The final tree was visualised using iTOL (54).

508

509 RT-PCR of *yejABEF* cluster

510 All kits were used as per the manufacturer's instructions. Total RNA was
511 extracted from *A. tumefaciens* C58 WT using the RNeasy Plus Mini Kit (QIAGEN),
512 DNA was degraded using the TURBO DNA-free kit (Thermo) and cDNA was
513 synthesised using the Maxima Reverse Transcriptase (Thermo). PCR was
514 performed with primers FCP6349-6357 using the VeriFi polymerase (PCRBIO), with
515 a 64 °C annealing temperature and 1.5 min elongation time.

516

517 Transposon Sequencing

518 For identification of conditionally essential genes, transposon sequencing (Tn-
519 Seq) was performed broadly as described elsewhere (55), adapted for *A.*
520 *tumefaciens*. $3\text{-}5x10^5$ transposon mutants were generated per library by conjugation
521 of *A. tumefaciens* C58 with *E. coli* SM10λ-pir carrying the mariner transposon donor
522 plasmid pSC189 (56). Mutant libraries were selected on LB plates with 500 µg/mL
523 kanamycin (to select for the transposon), 25 µg/mL streptomycin (to remove the
524 donor *E. coli*) and 2 mg/mL Fosfomycin where appropriate. The libraries were
525 collected, genomic DNA extracted, and pooled genomic DNA fragments were
526 sequenced using a MiSeq system (Illumina). Insertion sites were identified and
527 statistical representation of transposon insertions determined using the ConArtist
528 pipeline as described (57).

Acknowledgements

We thank all members of the Cava lab for helpful comments and suggestions. Research in the Cava lab is supported by the Swedish Research Council, the Laboratory for Molecular Infection Medicine Sweden (MIMS), Umeå University, the Knut and Alice Wallenberg Foundation (KAW) and the Kempe Foundation.

References

1. W. Vollmer, D. Blanot, M. A. De Pedro, Peptidoglycan structure and architecture. *FEMS Microbiology Reviews* **32**, 149–167 (2008).

2. W. Vollmer, B. Joris, P. Charlier, S. Foster, Bacterial peptidoglycan (murein) hydrolases. *FEMS Microbiology Reviews* **32**, 259–286 (2008).

3. O. Irazoki, S. B. Hernandez, F. Cava, Peptidoglycan muropeptides: Release, perception, and functions as signaling molecules. *Frontiers in Microbiology* **10** (2019).

4. J. T. Park, T. Uehara, How Bacteria Consume Their Own Exoskeletons (Turnover and Recycling of Cell Wall Peptidoglycan). *Microbiology and Molecular Biology Reviews* **72**, 211–227 (2008).

5. C. Jacobs, L. J. Huang, E. Bartowsky, S. Normark, J. T. Park, Bacterial cell wall recycling provides cytosolic muropeptides as effectors for β-lactamase induction. *EMBO Journal* **13**, 4684–4694 (1994).

6. C. Jacobs, *et al.*, AmpD, essential for both β-lactamase regulation and cell wall recycling, is a novel cytosolic N-acetylmuramyl-L-alanine amidase. *Molecular Microbiology* **15**, 553–559 (1995).

7. M. F. Templin, A. Ursinus, J. V. Höltje, A defect in cell wall recycling triggers autolysis during the stationary growth phase of Escherichia coli. *EMBO Journal* **18**, 4108–4117 (1999).

8. J. Gisin, A. Schneider, B. Nägele, M. Borisova, C. Mayer, A cell wall recycling shortcut that bypasses peptidoglycan de novo biosynthesis. *Nature Chemical Biology* **9**, 491–493 (2013).

9. M. Borisova, J. Gisin, C. Mayer, The N-Acetylmuramic Acid 6-Phosphate Phosphatase MupP Completes the Pseudomonas Peptidoglycan Recycling Pathway Leading to Intrinsic Fosfomycin Resistance. *mBio* **8**, e00092-17 (2017).

10. C. Fumeaux, T. G. Bernhardt, Identification of MupP as a new peptidoglycan recycling factor and antibiotic resistance determinant in pseudomonas aeruginosa. *mBio* **8**, 1–13 (2017).

11. D. Mengin-Lecreulx, J. Van Heijenoort, J. T. Park, Identification of the mpl gene encoding UDP-N-acetylmuramate: L-alanyl- γ-D-glutamyl-meso-diaminopimelate ligase in Escherichia coli and its role in recycling of cell wall peptidoglycan. *Journal of Bacteriology* **178**, 5347–5352 (1996).

12. E. W. Goodell, Recycling of murein by Escherichia coli. *Journal of Bacteriology* **163**, 305–310 (1985).

13. E. Goodell, U. Schwarz, Release of Cell Wall Peptides into Culture Medium by Exponentially Growing Escherichia coli. *Journal of Bacteriology* **162**, 391–397 (1985).

14. S. B. Hernández, T. Dörr, M. K. Waldor, F. Cava, Modulation of Peptidoglycan Synthesis by Recycled Cell Wall Tetrapeptides. *Cell Reports* **31** (2020).

566 15. F. M. Kahan, J. S. Kahan, P. J. Cassidy, H. Kropp, The Mechanism of Action of Fosfomycin (Phosphonomycin). *Annals*
567 *of the New York Academy of Sciences* **235**, 364–386 (1974).

568 16. P. Seweryn, *et al.*, Structural insights into the bacterial carbon-phosphorus lyase machinery. *Nature* **525**, 68–72 (2015).

569 17. A. K. White, W. W. Metcalf, Microbial metabolism of reduced phosphorus compounds. *Annual Review of Microbiology*
570 **61**, 379–400 (2007).

571 18. J. W. McGrath, F. Hammerschmidt, J. P. Quinn, Biodegradation of phosphonomycin by Rhizobium huakuii PMY1.
572 *Applied and Environmental Microbiology* **64**, 356–358 (1998).

573 19. M. Novikova, *et al.*, The Escherichia coli Yej transporter is required for the uptake of translation inhibitor microcin C.
574 *Journal of Bacteriology* **189**, 8361–8365 (2007).

575 20. Q. Nicoud, *et al.*, Sinorhizobium meliloti Functions Required for Resistance to Antimicrobial NCR Peptides and Bacteroid
576 Differentiation. *mBio* **12**, e00895-21 (2021).

577 21. W. M. Figueroa-Cuilan, *et al.*, Induction of AmpC-Mediated β-Lactam Resistance Requires a Single Lytic
578 Transglycosylase in Agrobacterium tumefaciens. *Appl Environ Microbiol*, e0033322 (2022).

579 22. C. Jacobs, J.-M. Frère, S. Normark, Cytosolic Intermediates for Cell Wall Biosynthesis and Degradation Control
580 Inducible β-Lactam Resistance in Gram-Negative Bacteria. *Cell* **88**, 823–832 (1997).

581 23. A. Aliashkevich, F. Cava, LD-transpeptidases: the great unknown among the peptidoglycan cross-linkers. *FEBS Journal*
582 (2021) https:/doi.org/10.1111/febs.16066.

583 24. E. K. Perry, D. K. Newman, The transcription factors ActR and SoxR differentially affect the phenazine tolerance of
584 Agrobacterium tumefaciens. *Mol Microbiol* **112**, 199–218 (2019).

585 25. T. Muth, *et al.*, JDet: Interactive calculation and visualization of function-related conservation patterns in multiple
586 sequence alignments and structures. *Bioinformatics* **28**, 584–586 (2012).

587 26. I. G. Boneca, The role of peptidoglycan in pathogenesis. *Curr Opin Microbiol* **8**, 46–53 (2005).

588 27. R. E. Schaub, J. P. Dillard, The Pathogenic Neisseria Use a Streamlined Set of Peptidoglycan Degradation Proteins for
589 Peptidoglycan Remodeling, Recycling, and Toxic Fragment Release. *Frontiers in Microbiology* **10** (2019).

590 28. R. S. Rosenthal, W. Nogami, B. T. Cookson, W. E. Goldman, W. J. Folkening, Major fragment of soluble peptidoglycan
591 released from growing Bordetella pertussis is tracheal cytotoxin. *Infection and Immunity* **55**, 2117–2120 (1987).

592 29. S. Mattoo, J. D. Cherry, Molecular Pathogenesis, Epidemiology, and Clinical Manifestations of Respiratory Infections
593 Due to Bordetella pertussis and Other Bordetella Subspecies. *Clin Microbiol Rev* **18**, 326–382 (2005).

594 30. Y. Dai, V. Pinedo, A. Y. Tang, F. Cava, E. Geisinger, A New Class of Cell Wall-Recycling l,d-Carboxypeptidase
595 Determines β-Lactam Susceptibility and Morphogenesis in Acinetobacter baumannii. *mBio* **12**, e0278621 (2021).

596 31. B. W. Simpson, *et al.*, Acinetobacter baumannii Can Survive with an Outer Membrane Lacking Lipooligosaccharide Due
597 to Structural Support from Elongasome Peptidoglycan Synthesis. *mBio* **12**, e0309921 (2021).

598 32. P. J. B. Brown, *et al.*, Polar growth in the Alphaproteobacterial order Rhizobiales. *Proceedings of the National Academy*
599 *of Sciences of the United States of America* **109**, 1697–1701 (2012).

600 33. E. Krol, *et al.*, Tol-Pal System and Rgs Proteins Interact to Promote Unipolar Growth and Cell Division in Sinorhizobium
601 meliloti. *mBio* **11**, e00306-20 (2020).

602 34. A. I. Weaver, *et al.*, Lytic transglycosylases mitigate periplasmic crowding by degrading soluble cell wall turnover
603 products. *Elife* **11**, e73178 (2022).

604 35. M. W. Breedveld, K. J. Miller, Cyclic beta-glucans of members of the family Rhizobiaceae. *Microbiol Rev* **58**, 145–161
605 (1994).

606 36. S. Giacomucci, L. Alvarez, C. D. A. Rodrigues, F. Cava, C. Paradis-Bleau, Hydroxyl Radical Overproduction in the
607 Envelope: an Achilles' Heel in Peptidoglycan Synthesis. *Microbiol Spectr* **10**, e0120321 (2022).

608 37. M. F. F. Arnold, *et al.*, Genome-Wide Sensitivity Analysis of the Microsymbiont Sinorhizobium meliloti to Symbiotically
609 Important, Defensin-Like Host Peptides. *mBio* **8**, e01060-17 (2017).

610 38. T. H. Mauchline, *et al.*, Mapping the Sinorhizobium meliloti 1021 solute-binding protein-dependent transportome.
611 *Proceedings of the National Academy of Sciences* **103**, 17933–17938 (2006).

612 39. J. P. W. Young, *et al.*, The genome of Rhizobium leguminosarum has recognizable core and accessory components.
613 *Genome Biology* **7**, R34 (2006).

614 40. J. Prell, *et al.*, The PTSNtr system globally regulates ATP-dependent transporters in Rhizobium leguminosarum.
615 *Molecular Microbiology* **84**, 117–129 (2012).

616 41. V. Untiet, *et al.*, ABC transport is inactivated by the PTS(Ntr) under potassium limitation in Rhizobium leguminosarum
617 3841. *PLoS One* **8**, e64682 (2013).

618 42. G. Mulley, *et al.*, Mutation of GOGAT prevents pea bacteroid formation and N2 fixation by globally downregulating
619 transport of organic nitrogen sources. *Mol Microbiol* **80**, 149–167 (2011).

620 43. G. Cheng, R. Karunakaran, A. K. East, O. Munoz-Azcarate, P. S. Poole, Glutathione affects the transport activity of
621 Rhizobium leguminosarum 3841 and is essential for efficient nodulation. *FEMS Microbiol Lett* **364** (2017).

622 44. J. Hartl, *et al.*, Untargeted metabolomics links glutathione to bacterial cell cycle progression. *Nat Metab* **2**, 153–166
623 (2020).

624 45. E. R. Morton, C. Fuqua, Laboratory Maintenance of Agrobacterium. *Current Protocols in Microbiology* **73**, 141–151
625 (2012).

626 46. E. R. Morton, C. Fuqua, Genetic manipulation of Agrobacterium. *Current Protocols in Microbiology*, 1–15 (2012).

627 47. L. Alvarez, S. B. Hernandez, M. A. De Pedro, F. Cava, "Ultra-Sensitive, High-Resolution Liquid Chromatography
628 Methods for the High-Throughput Quantitative Analysis of Bacterial Cell Wall Chemistry and Structure" in *Bacterial Cell*
629 *Wall Homeostasis: Methods and Protocols*, (2016).

630 48. F. Cava, M. A. De Pedro, H. Lam, B. M. Davis, M. K. Waldor, Distinct pathways for modification of the bacterial cell wall
631 by non-canonical D-amino acids. *EMBO Journal* **30**, 3442–3453 (2011).

632 49. M. N. Price, *et al.*, Mutant phenotypes for thousands of bacterial genes of unknown function. *Nature* **557**, 503–509
633 (2018).

634 50. J. Huerta-Cepas, *et al.*, eggNOG 5.0: a hierarchical, functionally and phylogenetically annotated orthology resource
635 based on 5090 organisms and 2502 viruses. *Nucleic Acids Research* **47**, D309–D314 (2019).

636 51. R. C. Edgar, MUSCLE: multiple sequence alignment with high accuracy and high throughput. *Nucleic Acids Research*
637 **32**, 1792–1797 (2004).

638 52. G. E. Crooks, G. Hon, J.-M. Chandonia, S. E. Brenner, WebLogo: a sequence logo generator. *Genome Res* **14**, 1188–
639 1190 (2004).

640 53. E. V. Kriventseva, *et al.*, OrthoDB v10: sampling the diversity of animal, plant, fungal, protist, bacterial and viral
641 genomes for evolutionary and functional annotations of orthologs. *Nucleic Acids Research* **47**, D807–D811 (2019).

642 54. I. Letunic, P. Bork, Interactive Tree Of Life (iTOL) v5: an online tool for phylogenetic tree display and annotation. *Nucleic*
643 *Acids Research* **49**, W293–W296 (2021).

644 55. M. C. Chao, *et al.*, High-resolution definition of the Vibrio cholerae essential gene set with hidden Markov model-based
645 analyses of transposon-insertion sequencing data. *Nucleic Acids Research* **41**, 9033–9048 (2013).

646 56. S. L. Chiang, E. J. Rubin, Construction of a mariner-based transposon for epitope-tagging and genomic targeting. *Gene*
647 **296**, 179–185 (2002).

648 57. J. R. Pritchard, *et al.*, ARTIST: High-Resolution Genome-Wide Assessment of Fitness Using Transposon-Insertion
649 Sequencing. *PLoS Genetics* **10** (2014).

650

Figures

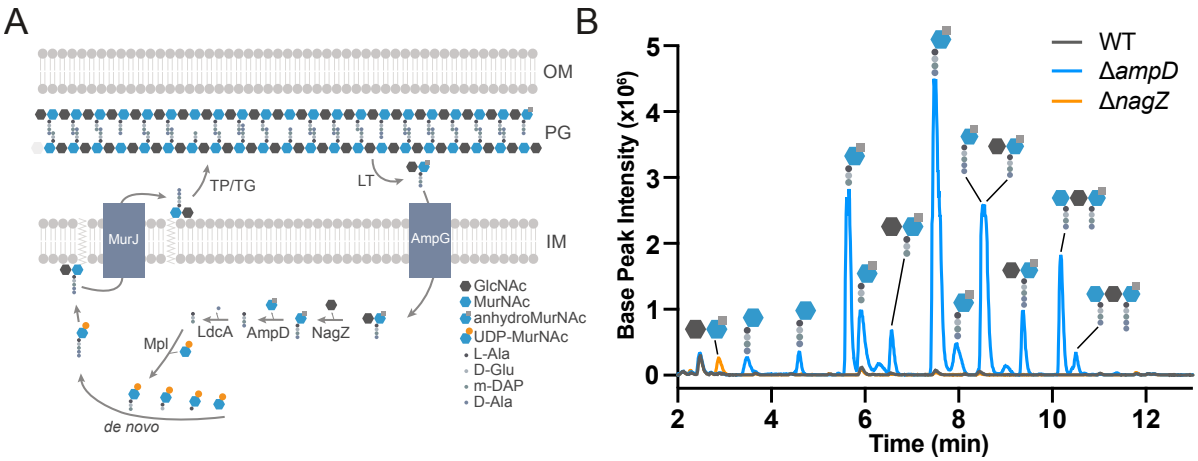

Figure 1. *A. tumefaciens* recycles muropeptides. (A). Schematic diagram of PG recycling pathway in *E. coli*. TP, transpeptidase; TG, transglycosylase; LT, lytic transglycosylase; OM, outer membrane; PG, peptidoglycan; IM, inner membrane. (B). Soluble PG fragments that accumulate in the cytoplasm of *A. tumefaciens* WT, Δ*ampD* and Δ*nagZ* strains detected using LC-MS.

659

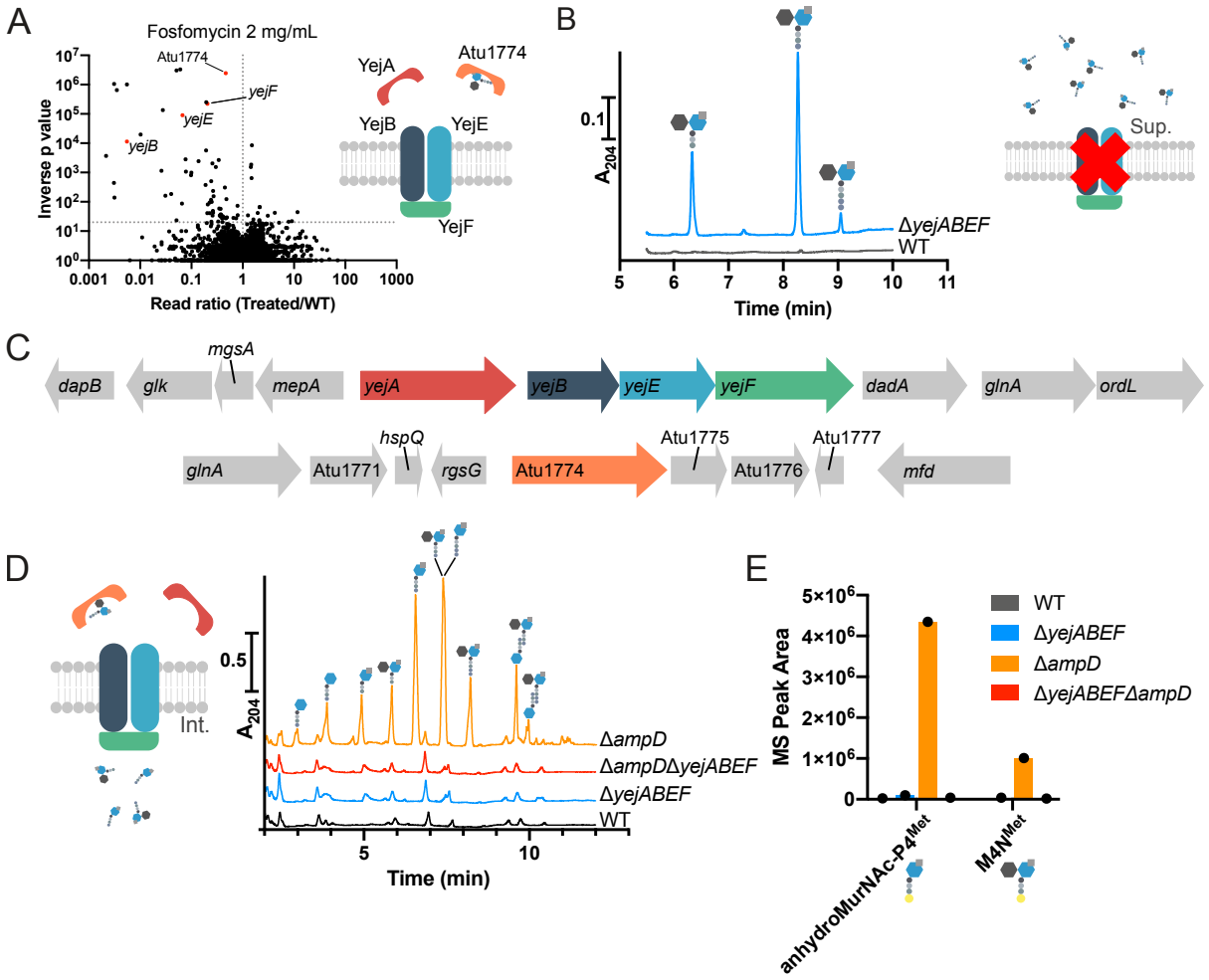

660

661 Figure 2. YejBEF is the PG recycling transporter in *A. tumefaciens*. (A). Volcano plot
662 showing the ratio of Transposon sequencing (Tn-Seq) reads mapped to genes in the
663 *A. tumefaciens* WT strain treated with 2 mg/mL Fosfomycin compared to control,
664 plotted against inverse p-value. Genes corresponding to *yejBEF* and Atu1774 are
665 highlighted in red. (B). UPLC chromatogram showing levels of anhydromuropeptides
666 released into the supernatants by *A. tumefaciens* WT and Δ*yejABEF* strains (C).
667 Genomic context of *yejABEF* and Atu1774. (D). Soluble PG fragments that
668 accumulate in *A. tumefaciens* WT, Δ*yejABEF*, Δ*ampD* and Δ*yejABEF*Δ*ampD* strains
669 detected using UPLC.

670

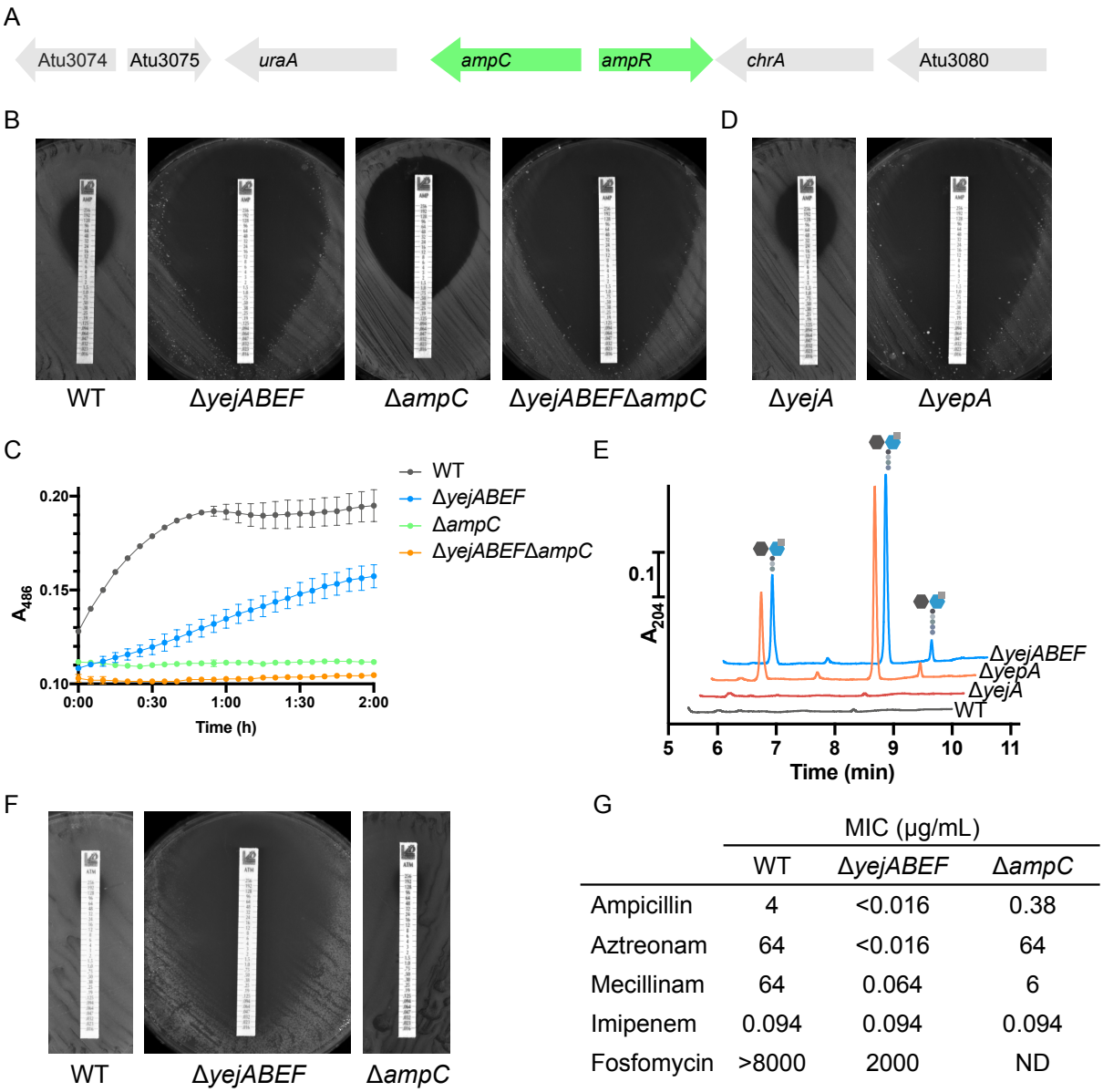

G

	MIC (μg/mL)		
	WT	Δ*yejABEF*	Δ*ampC*
Ampicillin	4	<0.016	0.38
Aztreonam	64	<0.016	64
Mecillinam	64	0.064	6
Imipenem	0.094	0.094	0.094
Fosfomycin	>8000	2000	ND

Figure 3. Δ*yejABEF* is hypersensitive to Ampicillin, in a manner only partly dependent on the β-lactamase AmpC. (A). Genomic context of the AmpC β-lactamase in A. tumefaciens, showing proximity to canonical AmpR repressor. (B). Comparison of Amp resistance of A. tumefaciens WT, Δ*yejABEF*, Δ*ampC* and Δ*yejABEF*Δ*ampC* strains by growth on LB plates with Ampicillin MIC test strips. (C). Hydrolysis of nitrocefin by lysates of *A. tumefaciens* WT, Δ*yejABEF*, Δ*ampC* and Δ*yejABEF*Δ*ampC* strains, measured by following A_{486}. (D). Comparison of Amp resistance of *A. tumefaciens* Δ*yejA* and Δ*yepA* strains. (E). Accumulation of

680 muropeptides in the supernatants of *A. tumefaciens* WT, ΔyepA, ΔyejA and
681 ΔyejABEF strains, measured by UPLC. (F). Comparison of Aztreonam resistance of
682 A. tumefaciens WT, Δ*yejABEF* and Δ*ampC* strains by growth on LB plates with
683 Aztreonam MIC test strips. (G). Minimal inhibitory concentration (MIC) values of A.
684 tumefaciens WT, Δ*yejABEF* and Δ*ampC* to β-lactams Ampicillin, Aztreonam,
685 Mecillinam, Imipenem, and MurA-inhibitor Fosfomycin.

686

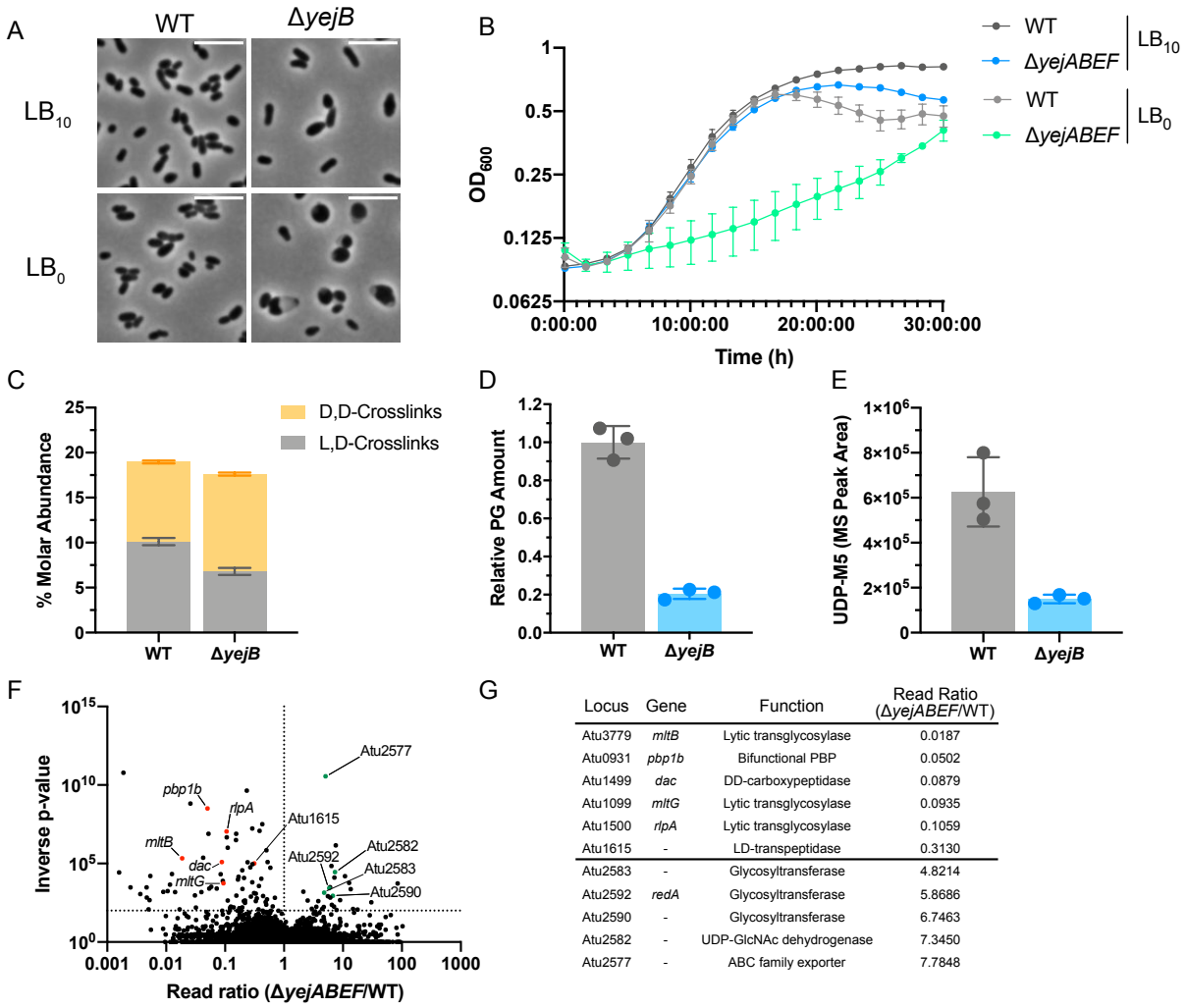

G

Locus	Gene	Function	Read Ratio (Δ*yejABEF*/WT)
Atu3779	*mltB*	Lytic transglycosylase	0.0187
Atu0931	*pbp1b*	Bifunctional PBP	0.0502
Atu1499	*dac*	DD-carboxypeptidase	0.0879
Atu1099	*mltG*	Lytic transglycosylase	0.0935
Atu1500	*rlpA*	Lytic transglycosylase	0.1059
Atu1615	-	LD-transpeptidase	0.3130
Atu2583	-	Glycosyltransferase	4.8214
Atu2592	*redA*	Glycosyltransferase	5.8686
Atu2590	-	Glycosyltransferase	6.7463
Atu2582	-	UDP-GlcNAc dehydrogenase	7.3450
Atu2577	-	ABC family exporter	7.7848

Figure 4. PG recycling is required for cell wall integrity in *A. tumefaciens*. (A-E). Phenotypic analysis of *A. tumefaciens* WT and Δ*yejABEF* strains. (A). Phase contrast microscopy of WT and Δ*yejB* cells grown on LB_{10} and LB_0. (B). Growth curves of WT and Δ*yejABEF* on LB_{10} and LB_0. (C). Molar abundance of DD- and LD-crosslinks in cell walls determined by UPLC analysis of WT and Δ*yejB* PG. (D). Relative PG amounts determined by total area under UPLC chromatograms of WT and Δ*yejB* PG. (E). LC-MS quantification of primary soluble PG precursor UDP-M5 in WT and Δ*yejB*. (F). Volcano plot showing the ratio of Tn-Seq reads mapped to genes in the *A. tumefaciens* Δ*yejABEF* strain compared to WT as control. Selected

698 synthetically detrimental (red) and synthetically beneficial (green) hits are

699 highlighted. (G). Table listing selected synthetically detrimental or beneficial hits in

700 Δ*yejABEF* Tn-Seq with annotations.

701

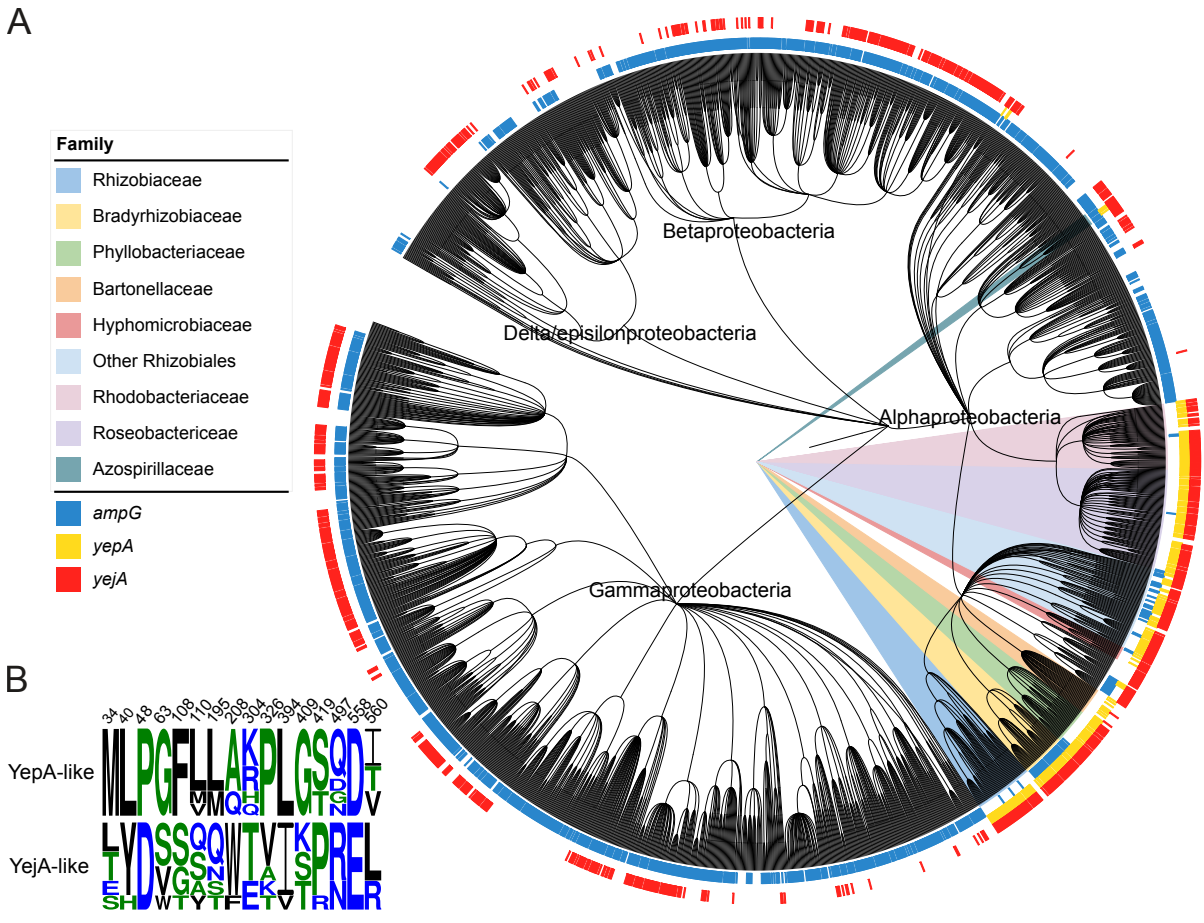

Figure 5. YejABEF is widespread in the proteobacteria, but YepA is only present in the Alphaproteobacteria. (A). Phylogenetic tree showing distribution of *ampG*, *yejA* and *yepA* in the proteobacteria. (B). Molecular fingerprint residues of YepA used to differentiate between YejA and YepA.

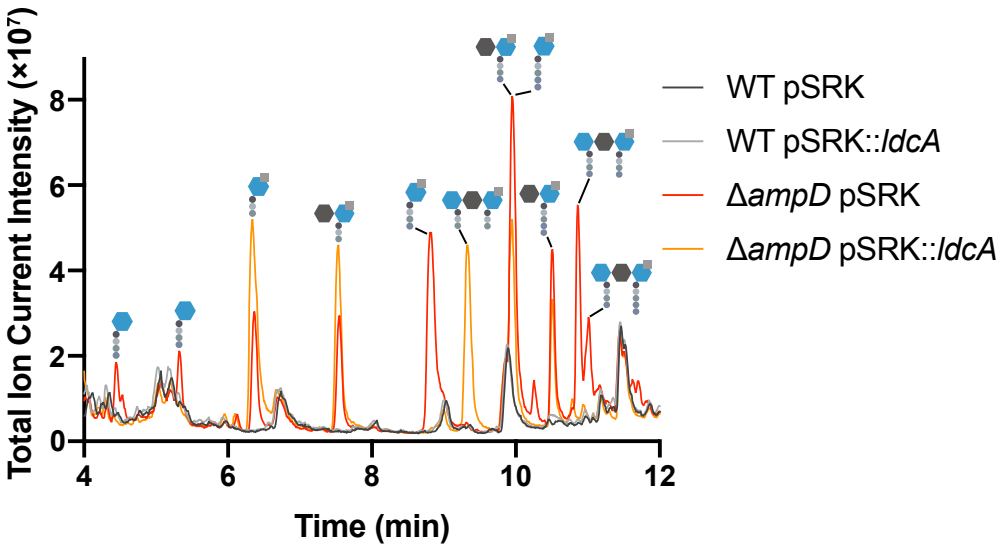

708

709 Supplementary Figure 1. Detection of accumulating muropeptide species in *A.*

710 *tumefaciens* WT and Δ*ampD* strains containing expression vector with or without *E.*

711 *coli ldcA* using LC-MS.

712

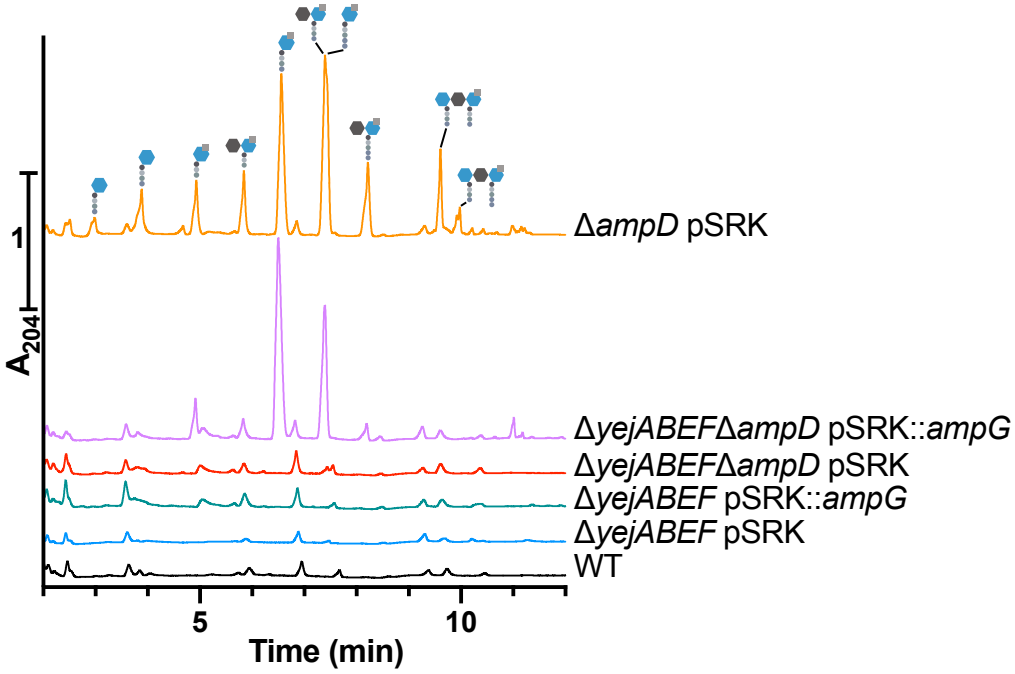

713

714 Supplementary Figure 2. Detection of accumulating muropeptide species in A.

715 tumefaciens WT, Δ*ampD*, Δ*yejABEF* and Δ*yejABEF*Δ*ampD* containing expression

716 vector with or without *E. coli ampG* using UPLC.

717

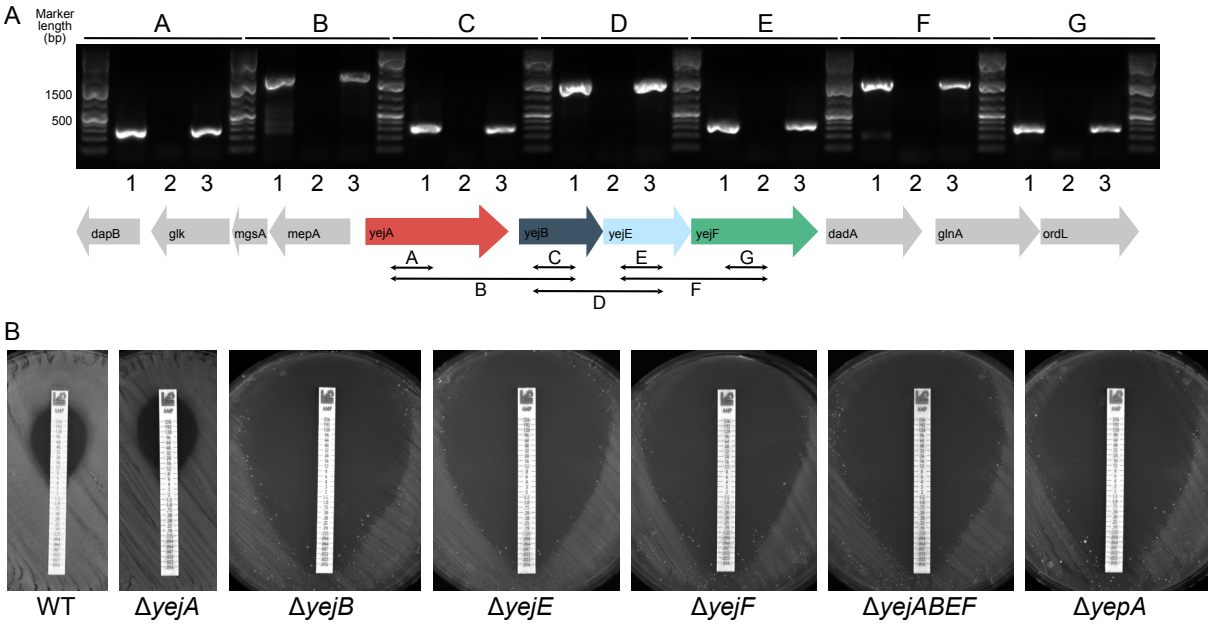

Supplementary Figure 3. *yejABEF* genes are co-transcribed, but yejA is not involved in PG recycling. (A). PCR amplification using as template: 1. gDNA; 2. RT reaction without added RT; 3. cDNA. Inter- and intragenic regions amplified are indicated below. (B). Ampicillin MIC test strips of *A. tumefaciens* WT, Δ*yejA*, Δ*yejB*, Δ*yejE*, Δ*yejF*, Δ*yejABEF* and Δ*yepA*.

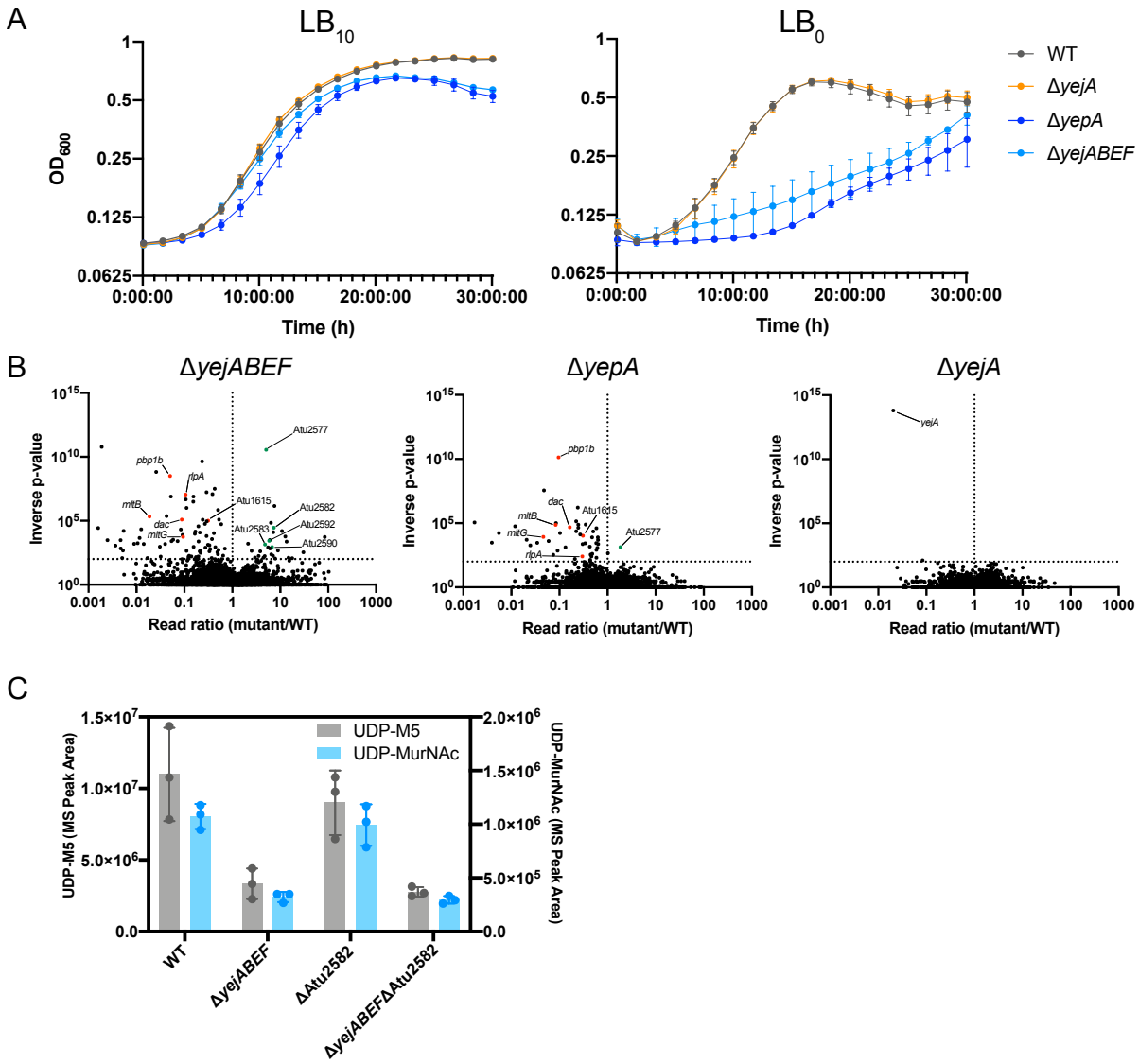

Supplementary Figure 4. PG recycling is required for cell wall integrity in *A. tumefaciens* (cont.). (A). Growth curves of *A. tumefaciens* WT, ΔyejA, ΔyepA and ΔyejABEF strains on LB_{10} and LB_0. (B). Volcano plot showing the ratio of Tn-Seq reads mapped to genes in the *A. tumefaciens* Δ*yejABEF*, Δ*yepA* and Δ*yejA* strains compared to WT as control. Selected synthetically detrimental (red) and synthetically beneficial (green) hits are highlighted. (C) Quantification of PG precursors UDP-M5 and UDP-MurNAc in *A. tumefaciens* WT, Δ*yejABEF*, ΔAtu2582 and Δ*yejABEF*ΔAtu2582 strains using LC-MS.